Lab on a Chip

Miniaturisation for chemistry, physics, biology, & bioengineering

www.rsc.org/loc

Volume 9 | Number 16 | 21 August 2009 | Pages 2253–2408

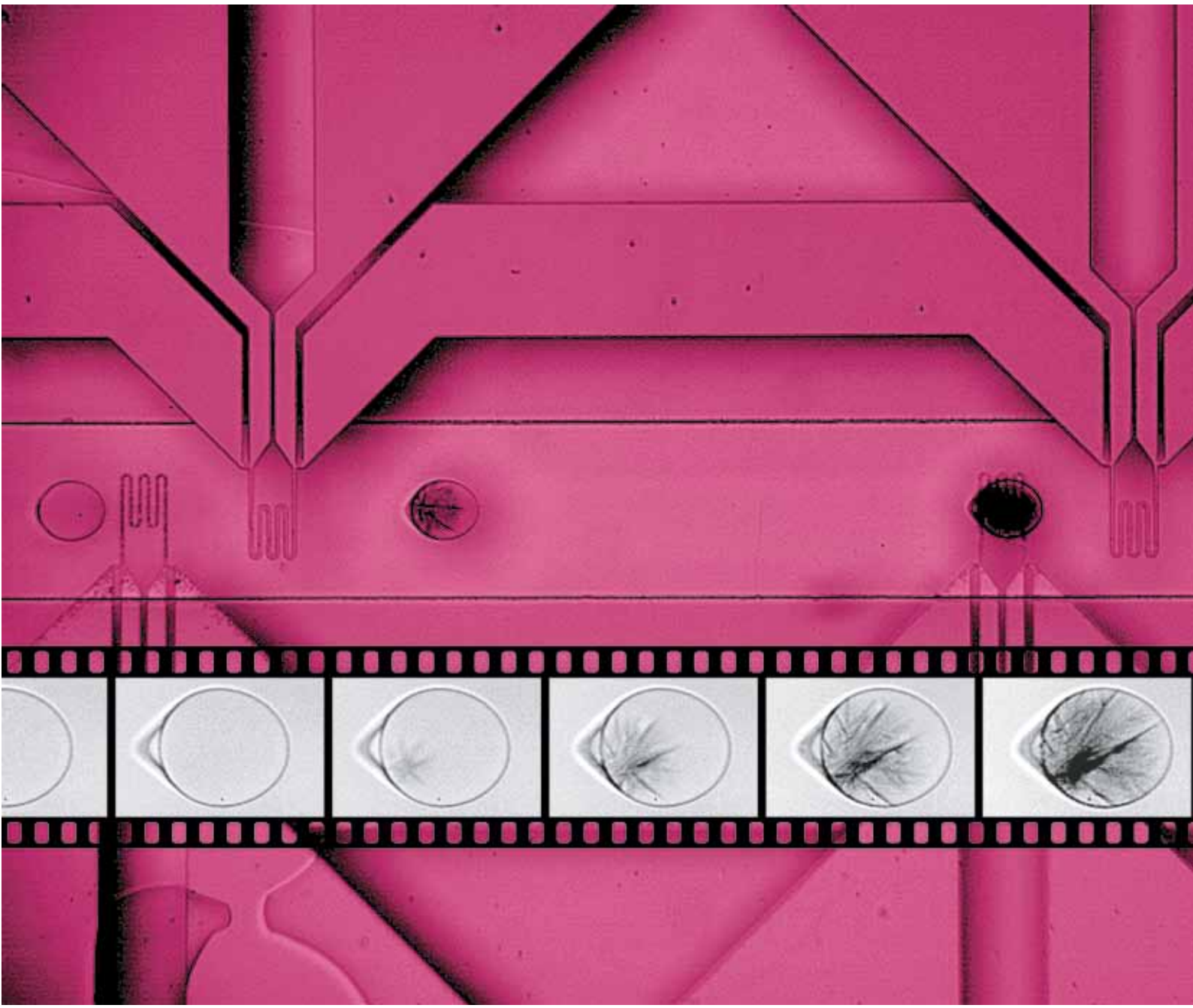

ISSN 1473-0197

Whitesides
Ice nucleation in supercooled water

Ismagilov
SlipChip

den Toonder
Artificial cilia micro-mixer

Jo and Schwartz
Stretching DNA molecules

RSC Publishing

1473-0197(2009)9:16;1-U

A microfluidic apparatus for the study of ice nucleation in supercooled water drops†

Claudiu A. Stan,[a] Grégory F. Schneider,[a] Sergey S. Shevkoplyas,[a] Michinao Hashimoto,[a] Mihai Ibanescu,[b] Benjamin J. Wiley[a] and George M. Whitesides*[a]

Received 30th March 2009, Accepted 1st May 2009
First published as an Advance Article on the web 22nd May 2009
DOI: 10.1039/b906198c

This paper describes a microfluidic instrument that produces drops of supercooled water suspended in a moving stream of liquid fluorocarbon, and measures the temperatures at which ice nucleates in the drops. A microfluidic chip containing a monodisperse drop generator and a straight channel with 38 embedded resistance thermometers was placed in contact with a seven-zone temperature-control plate and imaged under a microscope with a high-speed camera. This instrument can record the freezing temperatures of tens of thousands of drops within minutes, with an accuracy of 0.4 °C. The ice-nucleation temperatures in ~80-μm drops were reported for the freezing of 37 061 drops of pure water, and of 8898 drops of water seeded with silver iodide. Nucleation of ice in pure water was homogenous and occurred at temperatures between −36 and −37.8 °C, while water containing silver iodide froze between −10 and −19 °C. The instrument recorded the largest sets of individual freezing temperatures (37 061), had the fastest data acquisition rate (75 measurements/s), and the best optical (3 μm) and temporal (70 μs) resolutions among instruments designed to study nucleation of ice. The dendritic growth of ice in 150-μm drops of supercooled water at −35 °C was observed and imaged at a rate of 16 000 frames/s.

Introduction

This paper describes the development of a microfluidic apparatus for the production and study of drops of supercooled water suspended in a stream of perfluoromethyldecalin, and flowing in a microfluidic channel. We designed this apparatus to measure the freezing temperatures of large ensembles of identical supercooled drops of water at very high repetition rates. The apparatus produces long sequences (>30 000) of small drops of supercooled water (~100-μm diameter) by cooling drops of water below 0 °C. The drops freeze when ice (the thermodynamically stable phase) nucleates in supercooled water. The apparatus records the freezing temperature of each drop, at a rate up to 75 measurements per second; this is the highest rate of data acquisition reported to date. The apparatus is also a very reliable generator of supercooled water drops with temperatures down to −35 °C.

Understanding supercooling, and the nucleation of formation of ice in liquid water is important in a wide range of fields in science and technology: examples include determination of the fundamental physicochemical properties of water;[1] the formation and the properties of atmospheric precipitation;[2] icing on surfaces such as roads and aircraft wings; snowmaking for ski resorts; life at temperatures below 0 °C;[1] and the storage of reactive, or biologically active substances.[3–5]

Background

Small amounts of pure water (<1 μL volume) can be supercooled to below −35 °C before the homogenous nucleation of ice initiates its freezing.[1] In most circumstances, the lowest temperature to which samples of water can be supercooled is much above the temperatures at which homogenous nucleation is probable (−35 °C to −40 °C for small volumes of water[6]), because ice nucleates heterogeneously on the surface of its containers or on impurity particles (*e.g.*, dust) present in the water.[2]

A metastable liquid such as supercooled water can exist because its transition to the thermodynamically stable phase must start with the formation of a microscopic amount of the stable phase within the bulk metastable phase.[1] This first step (*i.e.* the nucleation) is energetically unfavorable because it involves the creation of a high free-energy interface between the two phases. External perturbations such as mechanical vibrations and impurities can provide the energy necessary for nucleation; this process is called heterogeneous nucleation. In the absence of external perturbations, the system can be taken further from equilibrium, but it will reach eventually a state in which thermally-driven, localized density fluctuations will cause the nucleation of the stable phase; this process is called homogenous nucleation. The transition from the metastable to the stable

[a]*Department of Chemistry and Chemical Biology, Harvard University, Cambridge, MA, 01238, USA. E-mail: gwhitesides@gmwgroup.harvard.edu*
[b]*OmniGuide, Inc., Cambridge, MA, 01239, USA*

† Electronic supplementary information (ESI) available: i) Tabulated data on the designs of microfluidic channels used for ice nucleation experiments, ii) drawings of the PRTD sensor arrays used for this project, iii) a description of the process of fabricating the PRTD sensor arrays, iv) the calibration procedure for the PRTD sensors, v) derivation of the equations used for the calculation of ice nucleation rates, vi) the generalization of these equations for the case in which the temperature of the channel fluctuates, vii) freezing temperature and cooling rate data for ice nucleation experiments on pure water, and seeded with silver iodide; and viii) six movies of freezing drops inside microfluidic channels. See DOI: 10.1039/b906198c

phase does not occur at a fixed temperature, as equilibrium phase transitions do.

Experimental characterization of an out-of-equilibrium transition requires the investigation of a statistical ensemble of systems rather than a single measurement. For nucleation of ice it is necessary to determine the freezing temperatures of many identical samples, or to make repeated measurements of the freezing temperature on the same sample.

Experimental setups for the study of ice nucleation. Previous experiments were usually performed on small volumes (<1 mL) of water to avoid contamination from impurities. One possibility is to use water inside glass capillaries; after careful cleaning and preparation of the glass, Mossop was able to reach temperatures below −30 °C.[7] A much better container for supercooled water is the bulk phase of a liquid insoluble in water. Using two liquids with densities above and below the density of water, water drops can be suspended at the interface between liquids and avoid any contact with solid container walls.[8] Using this method it was possible to observe the homogenous freezing of water around −35 °C.[9] In other variations of the liquid-container method, the water was emulsified into small drops onto a continuous phase of another liquid,[10–12] and the thermal properties of the emulsions were monitored using differential scanning calorimetry (DSC).

Some supercooled water experiments studied drops in air or other gases using cloud chambers. In this case water drops are formed by condensation from water vapor that was suddenly cooled by adiabatic decompression.[13–15] Cloud chamber experiments produce very small drops (1–10 μm) and reported freezing temperatures lower than −40 °C.[13,16] In another class of experiments using drops in air, water drops were allowed to fall through a gradient of decreasing temperatures.[17,18] Water drops were also frozen while being levitated in acoustic[19] and electrodynamic[20] traps. Both the free-falling drop and the electrodynamic trap setups could cool water to the homogenous freezing temperature (which we infer to be between −35 and −37 °C for 100-μm drops).

Experimental design

We had four criteria for the design: i) The apparatus had to supercool water drops reliably all the way to the homogenous freezing temperature, and avoid heterogeneous freezing due to the presence of impurities (dust, bubbles) or through contact with the walls of the container. Thus, the apparatus would be appropriate for investigation of both homogenous ice nucleation in clean water, and heterogeneous ice nucleation caused by impurities which were intentionally added to the water. ii) The formation, cooling, and freezing of drops had to be continuous and stable over tens of minutes while having a rapid rate (>10 drops/s) in order to produce large-number (>10 000 data) statistics in *single* experimental runs. iii) The absolute accuracy of the measurement of the freezing temperature of a drop had to be on the order of 1 °C or better. iv) The size of the drop and its rate of cooling had to be tunable, in order to investigate the kinetics of ice nucleation over a wide range of temperatures and drop volumes.

The core of the experimental design that we developed, shown in Fig. 1, was a flow-focusing drop generator[21] connected to a straight microfluidic channel. The flow-focusing generator produced spherical water drops inside a continuous phase of liquid fluorocarbon. After generation, the drops and the fluorocarbon traveled in a straight microfluidic channel. A cold plate, made of five segments which could each be stabilized at set temperatures down to −45 °C, cooled the microfluidic device. As they traveled, the drops cooled to temperatures below 0 °C before they froze. We observed and measured the position at which each of the drops froze using a microscope, and monitored

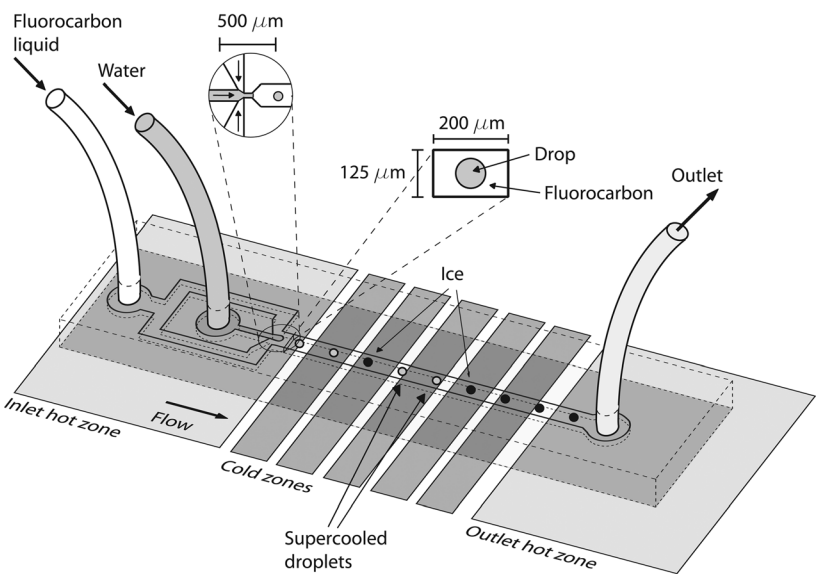

Fig. 1 Microfluidic apparatus for the study of ice nucleation in water. A microfluidic flow-focusing nozzle produced continuously drops of water in a stream of liquid fluorocarbon that carried the drops across the device. A seven-zone temperature-control plate cooled the chip such that the temperature of the drops gradually decreased until they froze. The position at which the drops froze was used to measure the temperature at which the freezing occurred.

the real-time distribution of temperature along the channel using arrays of thin-film resistance thermometers placed on the top and the bottom of the channel. We then used the distribution of temperature along the channel, and the positions at which the drops froze, to measure the freezing temperatures.

Using a liquid phase as the environment of the water drops allowed their mechanical and thermal manipulation using microfluidic technology. The liquid fluorocarbon that we used, pefluoromethyldecalin (PFMD), is chemically inert, has very low solubility in water, is compatible with many materials, and is not toxic. For the experiments we report here we had to use a fluorocarbon-soluble, and water-insoluble, surfactant ($CF_3(CF_2)_5CH_2CH_2OH$, THPFO) which was mixed with the PFMD at levels of 2:98 v:v. Because the drops do not touch the walls of the microfluidic channel, the microfluidic device can be built out of any material that is optically transparent and compatible with the fluids used in the experiment; for this work we used cross-linked polydimethylsiloxane (PDMS), soda-lime glass, and fused silica.

Results

Temperature control and measurement

The probability of freezing of a supercooled drop of pure water depends very steeply on temperature. Near −35 °C the freezing probability increases by a factor of about 50 as the temperature decreases by 1 °C.[6] Such a steep dependence makes quantitative evaluations of the freezing process difficult, and we took special care that the temperature control was stable, reliable, and flexible, and that the temperature measurement was sensitive and accurate.

Temperature control. The cooling of microfluidic devices, especially the cooling below 0 °C, is a relatively poorly developed part of microfluidic technology, with only a few experimental realizations up to the present.[22–25] We controlled the temperature of the channel by placing the glass side of the microfluidic device in contact with a temperature-control plate that had seven separate temperature-stabilized zones (Fig. 2). This design could deliver higher cooling power than on-chip cooling,[23] and was very reliable.

In principle, a single cold zone should be sufficient, by itself, to cause freezing, but we have discovered that for stable and reproducible conditions, it was necessary to have a minimum of three zones. The first zone, whose temperature was greater than 0 °C, assured that drops of water entered the channel at a known stable temperature. The second zone (cold) cooled the drops. The third zone (hot) melted the ice particles; if they were left solid, these particles clogged the outlet of the channel. We further divided the cold area of the plate into five smaller zones, whose temperature we could vary independently. The temperature-control plate thus had a total of seven independently-variable temperature zones, two hot and five cold.[26] This setup provided sensitive control over the temperature distribution along the channel.[27]

The method for cooling is a hybrid between liquid heat exchanging and thermoelectric cooling. We used miniature Peltier elements (Ferrotec 9503/035/025 M) to cool or heat the

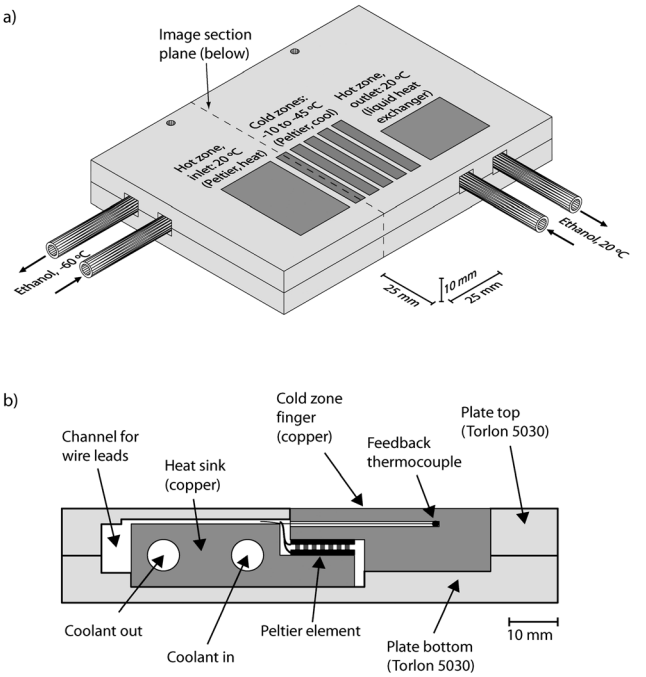

Fig. 2 Temperature control. a) Drawing (to scale) of the seven-zone temperature-control plate. The first six zones from left to right were controlled by Peltier elements embedded inside the plate; a liquid heat exchanger was used as heat sink for the elements. The seventh zone was a separate liquid heat exchanger, made smaller than first six to reduce heat loss. b) Cross-section (to scale) of the plate, showing its internal design.

first six zones; we changed the direction of the current in the Peltier elements to switch from cooling to heating. The heat sink for these elements was a common liquid heat exchanger which was embedded in the plate. We cooled the heat exchanger with ethanol from a cold-temperature bath (Lauda RP890C) that was set to −60 °C. This arrangement boosted the cooling capacity of the Peltier elements, such that we could achieve cold-zone temperatures down to −45 °C.[28] Commercial temperature controllers (Tempco TEC-220) regulated the amount of electrical power sent to the Peltier elements, such that the temperature of each zone could be set independently. Six controllers and the power supply for the Peltier elements were assembled into a single controller box for the plate. The second hot zone was a separate heat exchanger, pumped with ethanol at 20 °C which was supplied by a second temperature-controlled bath (VWR 1160S).

The minimum temperature we could stabilize was around −45 °C; the maximum temperature was higher than 50 °C.[29] The controllers had a setting and display resolution of 0.1 °C, and could stabilize exactly the temperatures of the cold zones to the set temperature (*i.e.* the temperatures could be stabilized to the desired values with fluctuations smaller than 0.1 °C). Before and after cooling, we set the temperatures of all zones near room temperature (~20 °C). Starting from room temperature, the plate could cool to the preset temperature values in approximately 10 minutes; heating back to room temperature took approximately 3 minutes.

Reduction of the vertical temperature gradient inside the channel. If the surface of the device was exposed to the ambient atmosphere during cooling, a significant vertical temperature difference (1–2 °C) developed between the top and the bottom of the channel. We blew cold nitrogen (~−25 °C) on top of the device to reduce the gradient, and to avoid frost formation from ambient water vapor. Three copper tubes, placed with even spacing on top of the device and aligned parallel to the channel, delivered the nitrogen. The nitrogen was cooled by a heat exchanger run by the same cold bath as the heat sink. The tubes (4 mm diameter) had sealed ends and were each drilled longitudinally in approximately 10 places, ensuring that the nitrogen flow was uniform across the top of the device. With top cooling added, the temperature difference was reduced to ~0.5 °C.

Temperature measurement with an array of thin-film platinum resistance thermometers. Our approach was to measure the temperature of our system by placing reliable and sensitive thermometers as close as possible to the drops, without disturbing the flow in the channel. We used linear arrays of thin-film platinum resistance temperature detectors (PRTD) which were embedded in the top and bottom walls of the channel. For our setup, thin-film PRTDs offered the best combination of temperature accuracy, temperature sensitivity, spatial resolution, and response time.

Fig. 3 shows the design of the PRTD linear array. We microfabricated these arrays on soda-lime glass or fused silica slides (50 × 75 × 1 mm) using lift-off lithography.[30] The fabrication procedure can be found in the ESI.† One array was fabricated directly on the glass slide that seals the PDMS slab, and the other array was fabricated on a smaller glass slide that was embedded in the PDMS slab. The arrays, which had 19 elements each and a 2.2 mm pitch, lined the top and the bottom surfaces of the channel. The high number of thermometers (38 if all were functioning) ensured that the temperature information had high spatial resolution, and that the overall measurement was tolerant to malfunctioning of a few PRTDs.[31]

A precision scanning digital multimeter (Keithley 2701 with two Keithley 7710 scanning cards) read individual PRTD resistances using a four-wire measurement method.[32] The multimeter read sequentially all PRTDs, at a rate of approximately 40 measurements per second; therefore the temperature values from all sensors were measured in approximately one second. This measurement cycle was repeated continuously during the experiments to provide real-time temperature measurement.

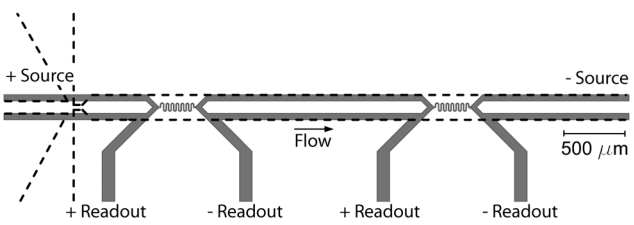

Fig. 3 Sensors for temperature measurement. Detail (to scale) of the temperature measurement system: an array of thin-film platinum resistance thermometers, embedded in the walls of the microfluidic channel. The thermometers and their connections for 4-wire measurements of resistance are shown in grey. The dashed line shows the outline of the microfluidic channel.

We calibrated the sensors against a factory-calibrated PRTD (Hart Scientific 5622-05, calibration accuracy ±0.04 °C). The stability of the calibration varied between sensor arrays fabricated in different batches. In the worst cases sensor arrays drifted by an average of 0.3 °C between calibrations; in the best cases these calibration drifts were as small as 0.01 °C. The ESI† contains further details on the calibration procedure.

For the data on pure water that we present in this paper, the sensor accuracy was ±0.21 °C; the best arrays that we tested had an accuracy of ±0.06 °C and a reproducibility of ±0.03 °C. The whole temperature readout system had a readout peak-to-peak noise of ±0.005 °C, and a sensitivity of 0.01 °C.

Construction and assembly of the microfluidic device

Design of a microfluidic drop generator and of a channel for freezing. Inside the microfluidic channel, the freezing of water drops often resulted in irregularly shaped ice particles. The drop generator and the channel had to be designed such that the ice particles did not jam inside the channel; jamming led to the clogging of the channel and the interruption of the experiment before large-number statistics could be acquired. We used spherical, and not disk-shaped, drops because spherical drops are less likely to jam inside the channel after freezing. The velocity of the drops had to be small enough that the drops would not deform (due to viscous shear) from a spherical shape; also, the velocity had to be large enough to avoid jamming. (The probability of jamming increased at small velocities.)

The insets in Fig. 1 show the design of the flow-focusing nozzle and of the channel which were used for freezing water drops. The flow-focusing nozzle was 125 μm tall, 40 μm wide, and 70 μm long. The straight channel had a rectangular cross section, with a width of 200 μm, a height of 125 μm, and a length of approximately 50 mm. The key feature of this design was the coupling of a nozzle with a high height-to-width ratio (~3:1) to a channel with a low height-to-width ratio (~1:2); this coupling allowed the generation of small spherical drops at relatively low rates of flow of the continuous phase. We achieved stable freezing with a few other device designs as well. Table ST-1 in the ESI† contains the details of these other designs.

Fabrication and assembly of the device with integrated thermometers. Fig. 4 illustrates the construction of the microfluidic

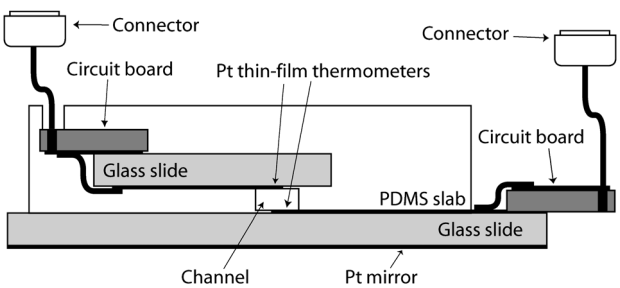

Fig. 4 Cross-sectional view (not to scale) of the microfluidic device. The thermometer arrays were patterned on glass slides, and the sensors were connected with thin gauge wire to two external connectors. One slide was embedded in the PDMS slab, and the other was bonded to the slab. The thin-film Pt mirror enhanced the contrast of the imaging.

device. We used soft lithographic techniques[33] to pattern the nozzle of the flow-focusing drop generator and the channel in a polydimethysiloxane (PDMS) slab. During the molding step, in which liquid PDMS was poured on top of a mold (made with photoresist on a silicone wafer), we immersed the first sensor array (patterned on a $\sim 25 \times 50 \times 1$ mm slide) in PDMS and pressed it against the mold such that the sensors were in contact with the channel part of the mold while the PDMS cured. We released the slab of cured PDMS ($\sim$5 mm thick) from the mold, plasma oxidized the slab, and covalently bond the slab to the second sensor array (patterned on a $50 \times 75 \times 1$ mm slide). The sensors of the second array were also aligned with the microfluidic channel, and thus the microfluidic device had two embedded arrays of sensors (one in the top wall, and one in the bottom wall). Lastly, the device was fitted with two high-density D-sub connectors (one for each sensor array) for easy connection to the temperature readout system.

Drop generation and transport

The choice of the liquid for the continuous phase. A main concern in choosing a continuous phase liquid for the freezing device was to avoid any influence of the continuous phase on the freezing process. In addition, the continuous phase had to support drop generation and transport at temperatures ranging from room temperature down to approximately -45 °C.

Our continuous phase was PFMD (pour point -70 °C), and the grade that we used (F2 Chemicals, batch number S0388B) was 97.9% pure; the impurity was mostly perfluorodecalin (PFD). These perfluorinated liquids have the advantage of being chemically inert, not toxic, compatible with many materials, and they have very low solubility in water and in hydrocarbons.

We added 2% (v:v) of THPFO (Sigma-Aldrich, 97%) to the continuous phase. THPFO reduces the interfacial tension between water and PFMD, and it stabilizes the generation and the transport of drops. We could not achieve stable drop generation with PFMD only, or at lower concentrations of THPFO. All three fluids in the carrier mixture are insoluble in water, with an estimated solubility[34] of 2.3×10^{-12} mol/L for PFMD, 9.6×10^{-11} mol/L for PFD, and 1.1×10^{-9} mol/L for THPFO.

Drop generation and transport. The microfluidic device could produce monodisperse drops of water under a range of rates of flow for water and PFMD. This allowed the generation of drops with different volumes (if the PFMD flow rate was changed), and at different frequencies of generation (if the water flow rate was changed). The velocity of the drops inside the channel had to be controlled as well, a task which is difficult in flow-focusing generators (a higher rate of flow decreases the size of the drops, but also increases their velocity). We solved this problem by varying the temperature of the flow-focusing nozzle to tune the size of the drops without changing their velocity.[35]

A typical set of operating parameters was: a nozzle temperature of approximately 20 °C, a water rate of flow of 0.065 mL/hr, and a PFMD rate of flow of 3.0 mL/hr.

Under these conditions the generator produced $\sim$80 μm diameter drops at a rate of $\sim$75 drops/s. The drop diameter was uniform, and we evaluated by imaging under a microscope that the relative standard deviation of the diameter was at most $\pm 1.2\%$.[36] The range of diameters for the drops that we could generate in the channel, and that froze reliably, spanned from 55 μm to 90 μm; we also generated and froze drops with diameters from 120 μm to 180 μm using larger channels. For all conditions suitable for freezing that we identified, the drop generation frequency varied from 20 drops/s to 200 drops/s. Table ST-1 in the ESI† lists the flow rate and nozzle temperature conditions under which these drops were generated.

Calculation of the temperature of the drops

The integrated microfabricated thermometers provided real-time knowledge of the temperatures along the top and bottom boundaries of the channel, and the drops traveled close to these boundaries (less than 100 μm away). To compute the drop temperature, we assumed that it sufficed to interpolate the temperature values along the boundaries of the channel. We nevertheless discovered that the low thermal diffusivity of PFMD (0.027 mm^2/s at room temperature), and an average velocity of flow of the PFMD in the channel on the order of $\sim$30 mm/s, resulted in large temperature gradients between the center of the channel and its boundaries. As the fluid cooled, the inside areas of the channel remained hotter than its periphery.

We therefore computed the drop temperatures using a two-step model. The first step was to calculate numerically the temperature distribution of the PFMD fluid in the absence of water drops. The model took into account longitudinal thermal transfer and the viscous-thermal coupling within the laminar flow of PFMD. For the second step we assumed that the temperature of the surface of the water drops is equal to the PFMD temperature calculated in the first step, and we calculated how the drop cooled while it traveled down the channel (and was in contact with increasingly colder PFMD). For this second step we assumed that the thermal transfer occurs by conduction only. Fig. 5 shows the results of the model for the two cooling conditions that we used for the data presented in this paper.

The numerical model did not consider the perturbation to the flow of liquid fluorocarbon due to the presence of the drops, nor the internal convection inside the water drops.[37] These simplifying assumptions could lead to errors in the calculation of the temperature of the drops that we could not evaluate analytically. Nevertheless, we were able to estimate experimentally that the error introduced by the model is less than 0.2 °C for cooling rates smaller than 20 °C/s as follows. The basic function of the model is to predict the temperature difference between the drops and the PRTDs, and this difference increases as the rate of cooling increases. Therefore we evaluated the error by comparing the calculated freezing temperatures for experiments in which the rate of cooling of the drops was different.

Optical observation of freezing at low and high imaging magnifications

Imaging setup. The temperature plate and the microfluidic device were thin enough to fit on a microscope stage. We imaged the microfluidic channel with a microscope (either a Leitz Orthoplan with 1.6× and 8× objectives, or a Nikon AZ100 with 0.5× and 5× objectives, and additional 1×–8× zoom). The

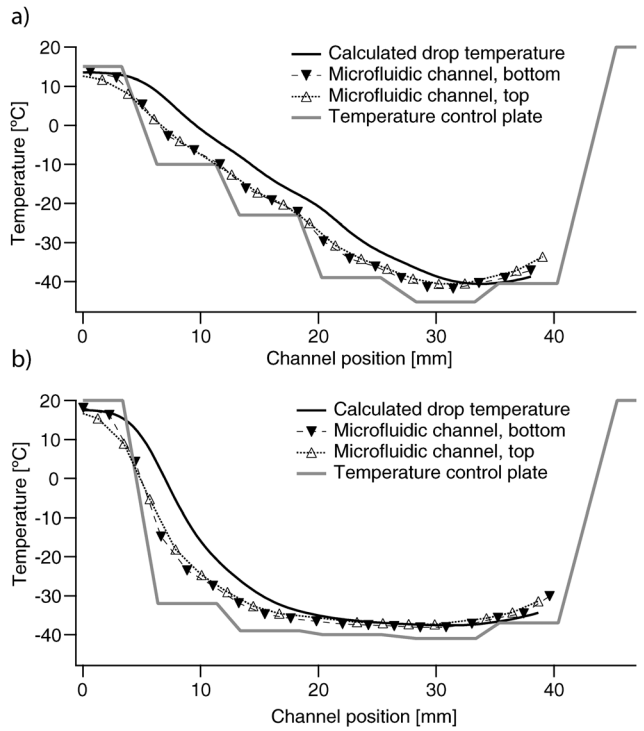

Fig. 5 The temperatures of the channel and of the drops inside the channel. The temperature distribution across the channel, measured with thermometer arrays embedded in the top and bottom walls of the channel, was used to model the temperature of the drops. a) Temperature setup for a constant cooling rate. b) Temperature setup for the freezing of pure water. The cooling rate in the region where freezing occurred (20 to 30 mm) was reduced approximately ten times to increase the accuracy of the measurements.

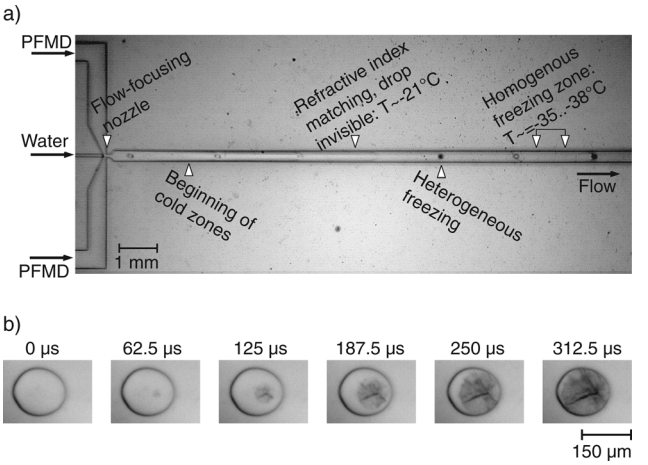

Fig. 6 Optical observation of freezing. a) Picture of the microfluidic device in operation; for clarity we show a device without PRTDs. Upon freezing, the image of the drops changed from a ring to a dark disk. b) High magnification pictures of a freezing drop, taken at a rate of 16 000 images/s. The pictures show the first stage of freezing, in which ice dendrites grew inside the drop at a velocity of approximately 30 cm/s. The times above the frames show the time elapsed since the first frame was recorded. The pictures in this figure were extracted from movies available in the ESI.†

miniaturization of our ice nucleation setup allowed us to take advantage of the capabilities of the microscope: aberration-corrected image formation, high resolution (better than 4.4 μm for 5× and 8× objectives[38]), variable magnification (0.5×–40×), and excellent efficiency of light collection. High-speed cameras (either Vision Research Phantom V7.3 with 8 Gb memory, or V9.1 with 1.5 Gb memory) recorded movies of the drops at a typical rate of 500 or 1000 frames per second, and a typical exposure time of 100 μs.

High-contrast optical detection of freezing at low magnification. We detected the freezing of the drops optically using reflected light microscopy. We coated the exposed side of the glass slide with an evaporated platinum mirror, so that areas of the device that did not scatter light (*e.g.* liquid drops) appeared bright, while areas of the device that scattered light (*e.g.* frozen drops) appeared dark. Fig. 6a shows drops freezing in a microfluidic channel. In between generation of the drop and its freezing, there was a place where the drops became barely visible because the oil we use (PFMD) became index-matched with supercooled water near −21 °C.

Our reflected-light imaging setup was simpler, and offered better imaging contrast than other optical freezing detection setups used in recent ice nucleation experiments,[18,20] which analyze the change in the polarization after light is scattered by ice. In addition to being scattered, the light which passes through a frozen drop also changes its state of polarization. In principle this change could be used to identify frozen drops, or at least to enhance the contrast of the image; we nevertheless found that the image quality was the same in the microscope that was not sensitive to the change in polarization (Leitz Orthoplan), as in the microscope that was sensitive (Nikon AZ100).

The key factor in achieving a high contrast was to use a low numerical aperture. We tested different microscope objectives, and the ones with lower numerical aperture generated the best contrast. The high imaging contrast allowed efficient automated image analysis of the movies of freezing drops for the extraction of freezing positions relative to the start of the channel.

High-resolution and high-speed imaging of the freezing process at high magnification. Using a higher magnification and a faster camera frame rate we could observe the freezing process with high temporal and spatial resolution. Fig. 6b shows a high-speed (16 000 frames/s) recording of the initial stages of freezing inside a 150-μm diameter drop, at a temperature of ∼−35 °C. The freezing of deeply supercooled water had two stages. During a fast first stage, ice dendrites grew rapidly (∼1 ms) inside the drop until the drop was filled with a mixture of water and ice crystals at a temperature close to 0 °C. During the second stage the remaining water froze slowly (∼30 ms), as heat was lost from the drop into the colder surrounding PFMD. We could observe both stages of freezing optically, and we could locate the point where nucleation occurred with a resolution (∼3 μm) equal to the pixel size of the image. The optical (∼3 μm) and temporal (∼70 μs) resolutions with which we could investigate optically the freezing process are, to our knowledge, the best ever reported; these resolutions are several times better than those achieved in a recent experiment that investigated freezing in acoustically

levitated drops using high-speed imaging.[19] The ESI† contains movies showing droplets freezing under different conditions, including the movies from which the images in figure 6 were imported.

Fast solidification by dendritic growth is characteristic to supercooled liquids in contact with an environment colder than their melting temperature.[39] To our knowledge, such dendritic growth has not been previously investigated experimentally in pure water at temperatures below −24 °C.[19,40] For the drop in Fig. 6b (temperature ~−35 °C), the dendrites grew at a velocity of approximately 30 cm/s; this speed is within the range predicted by models of dendritic growth of ice.[40]

Calculation of temperature-dependent ice nucleation rates

The basic data that the apparatus produced was the temperature at which freezing initiates in a drop, T_F (in °C), and the rate of change of the temperature at the same moment, $(dT/dt)_F$ (in °C/s). These two measurements, repeated for large (>10 000) ensembles of drops with identical volumes, generated enough data to calculate temperature-dependent rates of nucleation of ice in supercooled water.

The temperature data from the PRTDs was used to calculate the position-dependent distribution of the temperature, and of the cooling rate, for drops of water moving inside the channel. We could update this calculation approximately once every second (the minimum time required to read all sensors); nevertheless, since the temperature readings were stable over several seconds, we averaged the PRTD data. The criteria for choosing the duration for averaging was that the largest change in the temperature readings among all sensors was less than 0.1 °C; this duration was between 20 s and 60 s typically.

We developed software for image analysis that labeled, tracked, and evaluated the image darkness for all the drops in a movie; the freezing was detected as a sudden increase in the darkness of the drop. Except for setting parameters such as the threshold darkness for freezing, and for verification, no user input was necessary during processing.

The flexibility in setting the cooling ramps with the seven-zone plate, and the large field-of-view (~15 mm), allowed us to record movies in which almost all drops (>99%) froze within the field of view. In our apparatus, almost every drop yielded useful freezing information. If this were not the case, we would have had to record multiple movies, each movie imaging a different section of the channel. Data recording using a single movie also reduced the fluctuations in the conditions of the experiment.

In the general case of a large ensemble of supercooled drops the rate of freezing of a drop, R_F, can be defined by eq. (1),

$$R_F = \frac{1}{\delta t}\frac{N_F}{N_L} \tag{1}$$

where δt the observation time in seconds, N_F is the number of drops that freeze within δt, and N_L is the number of liquid supercooled drops at the beginning of investigation; the unit of rate is 1/s. The duration of observation δt should be short enough such that the number of frozen drops is much smaller than the number of supercooled drops.

The rates of ice nucleation can be calculated from the freezing temperature and the cooling rate. Assuming that the temperature of the channel is stable the following two functions can be evaluated numerically:

$$N_L(T) = \text{the number of liquid drops that cool down to the temperature } T \tag{2}$$

$$\left(\frac{dT}{dt}\right)(T) = \text{the rate of cooling (°C/s) of the drops as a function of temperature} \tag{3}$$

The temperature-dependent rate of freezing, $R_F(T)$, can be evaluated from these two functions using eq. (4),

$$R_F(T) = -\left(\frac{dT}{dt}\right)(T)\frac{1}{N_L(T)}\frac{d}{dT}(N_L(T)) \tag{4}$$

The details of the derivation of eq. (4), and its generalization for the case in which the temperature of the channel fluctuates, are listed in the ESI.†

The rate of freezing $R_F(T)$ as it was defined here is an empirical function. Assumptions about the statistical properties of the nucleation were not used in its derivation. The capability of the microfluidic freezing setup to measure freezing rates without additional assumptions is a benefit of using large experimental data sets. Such a capability is important for an ice nucleation apparatus as the statistical nature of heterogeneous ice nucleation remains unclear:[41,42] while some experiments suggest that freezing is stochastic and only its rate can be known at a given temperature,[43] other experiments suggest that heterogeneous nucleation is deterministic and occurs at a well-defined temperature.[44]

Observation of homogenous ice nucleation

The criterion for homogenous ice nucleation in supercooled pure water. Proving beyond any doubt that a sample of water freezes homogenously (*i.e.* ice nucleates only due to thermally-induced density fluctuations in supercooled water) is probably not possible with the present experimental techniques used for the investigation of ice nucleation. Nucleation is a molecular scale phenomenon, but current ice nucleation instruments, including ours, record a macroscopic variable – the temperature – to characterize the nucleation process.

Here we measured the rate at which ice nucleates as a function of temperature, and compared this rate with the ones reported by previous experiments on ice nucleation in pure water. If these rates were equal within experimental uncertainty, we took this equality as evidence for homogenous nucleation of ice.

Avoiding contamination by ice-nucleating impurities. A critical requirement for achieving homogenous ice nucleation in the supercooled water drops is to avoid contamination with foreign impurities that could nucleate ice in water. Such impurities could be present in the water used for experiments, or the water could be contaminated during handling (by atmospheric dust or by contact with different containers).

The water that we used in our freezing experiments was either supplied by an ultrapure water purification system (Millipore Milli-Q Advantage A10), or we used commercial high purity water (Burdick & Jackson 365-4). We did not observe any difference between the two sources of ultrapure water. For the

data reported here we used water from the Millipore purification system (electrical resistivity 18.2 MΩ cm, less than 5 ppb total organic content). To transfer, hold, and dispense the water we used, in order: a 100-mL borosilicate glass beaker (VWR 89000-200), 1000-μL barrier pipette tips (VWR 87001-700), 1.7-mL microcentrifuge tubes (Sorenson 16070), 1-mL polycarbonate syringes (Becton-Dickinson 309628), general-use hypodermic needles (Becton-Dickinson 305165), polyethylene tubing (Becton-Dickinson 427416), and the microfluidic device. The beaker was cleaned first in a base bath (saturated solution of KOH in isopropyl alcohol) then in an acid bath (concentrated H_2SO_4). Except for the microfluidic device and the beaker, all other items were used only one time, and just after removal from their packaging. During handling, we kept the water covered as for as long as possible in order to avoid contamination from atmospheric dust.

The rate of ice nucleation in supercooled pure water. Fig. 7 shows the raw freezing position data for 37 211 drops of pure water, and the temperature readout from the PRTD that was located 22 mm away from the nozzle. Three characteristics of the experiment can be observed in these data: i) synchronous fluctuations in temperature and the freezing positions, ii) no freezing at a few well-defined positions in the image, and iii) a string of freezing positions located at the farthest position down the channel.

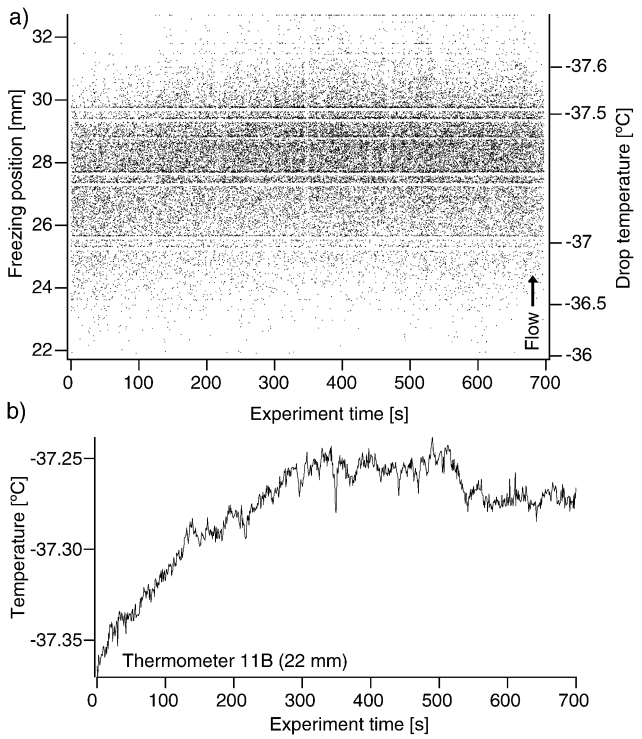

Fig. 7 a) The freezing positions of 37 211 drops of pure water as reported by image analysis software. The leads of the top sensors masked parts of the channel, and caused the horizontal strips where data is missing. The temperature scale is approximate because the temperature of the channel drifted during the experiment. b) Readout from the thermometer located at 22 mm. The temperature drifted in phase with the freezing positions.

The synchronous fluctuations of freezing positions and of the temperature of the channel show that freezing is temperature-dependent and that the temperature readout system operates correctly. These fluctuations occurred despite the fact that the temperatures of all zones were stable to better than 0.1 °C during the experiment, and illustrate the difficulty of evaluating the temperature in the channel. Without real-time temperature readout, it was not possible to measure with precision the temperature of the drops.

The irregularities in the freezing position data (the absence of freezing at specific locations and the freezing at the farthest position) were artifacts of the image analysis software. The lead wires for the top temperature sensors masked the area under them, and it was not possible to locate freezing under the leads. Nevertheless, the software recognized the freezing after the drops emerged from under the lead wires, and we smoothed the raw data by redistributing these freezing events uniformly over the masked areas. The freezing reported at the farthest position represents drops that exited the channel without freezing; accounting for these drops is important because they contribute to the total number of liquid drops (N_L in eq. (1)).

Ideally, the movies of freezing should cover enough of the length of the channel to catch all freezing events, and not much more because zooming out the image reduces its resolution. The statistical nature of the ice nucleation makes the choice of the field-of-view difficult because rare freezing events might occur far from the place where freezing typically occurs, and therefore will not be captured on movie. For the data in Fig. 7, 9 out of 37 211 drops entered the image frozen, and 141 exited the image still liquid. The number of drops that entered frozen is an upper bound for the amount of drops that do not freeze homogenously, and illustrates the high 'signal-to-noise' ratio that the instrument could achieve: fewer than one in 4000 drops froze at temperatures higher than −36 °C.

Fig. 8 shows the nucleation rate for pure water supplied by the Milli-Q filtration unit, calculated from the freezing temperatures of 34 267 drops from an ensemble of 37 211 drops of 79 μm diameter.[45] (The freezing temperatures for all these drops and their rate of cooling are available as a tab-delimited text computer file in the ESI.†) We calculated the temperature-dependent rate of ice nucleation, $J_N(T)$, using the functions $N_L(T)$ and $(dT/dt)(T)$ as described above, and starting from the formula:

$$J_N(T) = -\frac{1}{V_{drop}}\frac{1}{\delta t}\ln\left(\frac{N_L - N_F}{N_L}\right) \quad (5)$$

where $J_N(T)$ is the temperature-dependent rate of nucleation in $cm^{-3}\ s^{-1}$, V_{drop} the volume of the water drops in cm^3, and δt the time of observation in s. N_L and N_F are the numbers of liquid and freezing drops. The difference between the rate of freezing (eq. (1)) and the rate of nucleation, except for the normalization of the freezing rate by volume, is that in eq. (5) we assume the nucleation to be stochastic, which implies an exponential decay of N_L in time.[46]

We compared our ice nucleation rates against two previous sets of data: an average homogenous nucleation rate compiled using data from most ice nucleation experiments before 1995,[6] and results of a high-precision ice nucleation apparatus that levitates single drops in an electrodynamic trap.[47] The rates that

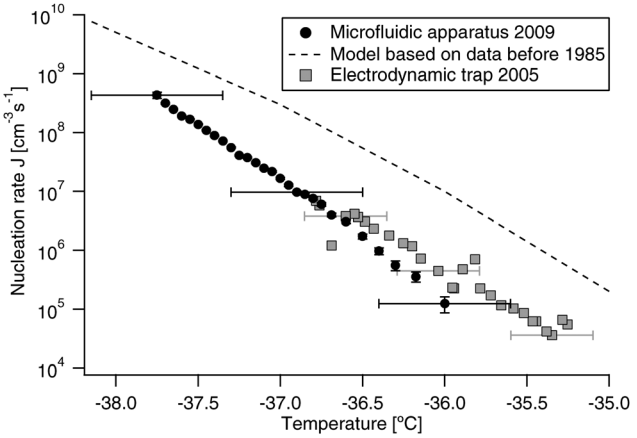

Fig. 8 Measurement of homogenous freezing rate in pure water using the microfluidic apparatus. The vertical error bars for the nucleation rate represent the statistical error caused by the use of a finite data set. The horizontal error bars represent the uncertainity of the temperature measurement. For comparison, we show a fit of experimental data that was available before 1995, and a recent high-precision measurement of the homogenous nucleation rate.

we measured are lower than the average of pre-1995 data, but are in very good agreement with data from the electrodynamic trap apparatus. Based on this comparison, we conclude that the ice nucleation that we observed is homogenous.

The rates of nucleation that we measured exhibit very little noise compared to previous experimental data.[6,47] This is in part a result of the high data throughput of our setup: the data ensemble that we present here is the largest ever reported for an ice nucleation experiment. Real-time temperature monitoring, and capturing in a single movie most of the freezing events that occur in the channel, also contribute to the low noise of the measurement. The statistical errors on the measurement of the rate are negligible because of the large amount of data. The most important source of uncertainty in our setup is the measurement of temperature; even though the accuracy of the temperature measurement is good (0.4 °C), the very steep dependence of the nucleation rate on temperature means that an error of only 0.5 °C in temperature measurement translates in a factor on the order of 10 in the nucleation rate.

Observation of heterogeneous ice nucleation induced by silver iodide colloids

Heterogeneous ice nucleation in supercooled water can be initiated by impurity particles present in water. This phenomenon occurs at higher temperatures (*i.e.* lower degrees of supercooling) than homogenous freezing, and is almost always responsible for the freezing of the larger volumes of water (larger than rain drops) found in nature.

The investigation of heterogeneous freezing requires more data than homogenous freezing, because the heterogeneous component (*e.g.* impurity particles) or condition (*e.g.* mechanical perturbations) adds experimental variables to the system. The data acquisition rates of current types of experiments are slow, and make it impractical to acquire statistically large sets of data.

We tested the suitability of our apparatus to the study of heterogeneous ice nucleation by introducing in the drops particles that can nucleate ice, and by measuring the freezing temperatures of these drops.[48]

Heterogeneous freezing of water by silver iodide. We used silver iodide nanoparticles (AgI NP) to nucleate ice. Silver iodide particles are particularly efficient at nucleating ice,[49] and their ice-nucleating properties have been measured experimentally many times. Therefore AgI NPs provided a good testing benchmark for our apparatus.

To synthesize AgI nanoparticles, KI (99.99%) and $AgNO_3$ (99.9999%) were purchased from Sigma-Aldrich. We added 10 μL of a 1 M aqueous KI solution, followed by 10 μL of a 1 M aqueous $AgNO_3$ solution, to 10 mL of deionized water. The water was mixed at high speed with a stir bar in a 20-mL borosilicate vial. After addition, the solution immediately turned yellowish-white due to the formation of AgI nanoparticles. The inset in Fig. 9b shows a scanning electron microscope (Zeiss Ultra55) of the AgI particles. The average diameter of the particles was 158 ± 44 nm, and it was determined by averaging over the size of 100 particles in microscope pictures.

Before feeding the solution of AgI NPs into the microfluidic device, we diluted it 2500 times in a 1 μM aqueous $AgNO_3$

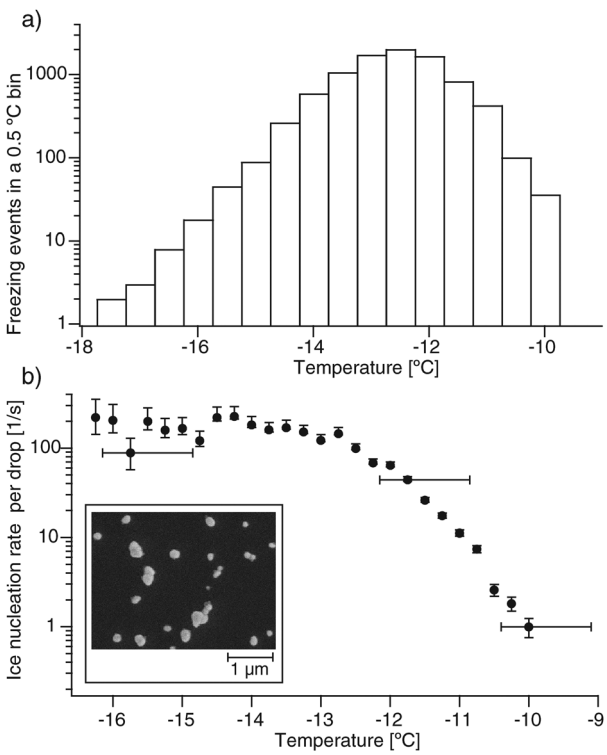

Fig. 9 Heterogeneous ice nucleation induced by silver iodide nanoparticles. a) Histogram of the freezing temperatures of 8898 drops containing silver iodide nanoparticles. b) The rate of ice nucleation per drop. The vertical error bars represent the statistical error of the nucleation rate plus the effect of neglecting the exponential decay of the number of unfrozen drops at a given temperature. The horizontal error bars indicate the uncertainity of the measurement of temperature; for clarity, only three temperature error bars are shown in the graph.

solution. We discovered that the freezing activity of the AgI NP solution was very sensitive to the amount of Ag^+ ions, and it was most active in the presence of 1 μM $AgNO_3$. This dependency was observed previously for AgI particles synthesized by other methods.[50,51] During synthesis, errors in weighing the reagents could easily lead to excess concentrations of either KI or $AgNO_3$ on the order of 1 μM; we therefore diluted the original AgI NP solution in 1 μM $AgNO_3$ to ensure reproducible conditions for nucleation.

Fig. 9a shows the histogram of freezing temperatures for 8898 drops containing AgI NPs out of a population of 8900 drops of 77 μm diameter. None of these drops froze at temperatures higher than −9.9 °C, and only two drops exited the investigation field-of-view not frozen (corresponding to cooling to approximately −19 °C). Fig. 9b shows the freezing rates per drop calculated from the freezing temperatures and cooling rates of 8890 drops.[52] Because the set of data was large, we could bin the freezing temperatures in narrow temperature intervals, and calculate the freezing rates without making the assumption that nucleation is stochastic. The difference between processing the data using eq. (1) (not stochastic) or eq. (5) (stochastic) was nevertheless minimal and is illustrated by the upper side of the error bars in Fig. 9b. The uncertainty of the measurement of temperature was larger than in the case of homogenous nucleation because the rate at which the drops cooled (approximately 100 °C/s) was fast. The freezing rate grows initially at an exponential rate as the temperature decreases, approximately by a factor of 8 for each degree Celsius lower in temperature. This increase is in qualitative agreement with previous measurements of heterogeneous nucleation rates induced by silver iodide.[43]

The leveling of the rate of freezing at temperatures below approximately −13 °C is surprising. It is nevertheless probable that this dependency does not reflect the true dependence of the heterogeneous nucleation rate. The average number of particles in a drop is small (on the order of 10) and it is possible that due to the stochastic Poisson distribution of the number of particles within drops, some drops do not contain ice-nucleating particles, or contain less active particles; these less active particles contribute to the flat part of the freezing rate curve. We note that using the particle diameter that we measured, we calculated an average number of AgI NPs per drop of approximately 2, and using the number of unfrozen drops we evaluated that the average number is on the order of 10. This large discrepancy was caused by the difficulty of measuring accurately the particle size distribution of the silver iodide nanoparticles.

Discussion

Comparison with other ice nucleation instruments

A variety of experimental techniques and instrumentation have been used to study the nucleation of ice in water.[53] Our instrument falls in the category of experiments that record freezing temperatures for each drop in an ensemble of drops. This category includes cold plate instruments,[41,42] drops in emulsions,[8,9] acoustic[19] or electrodynamic[20] levitating traps, and free-fall tubes.[17,18] Out of these, the electrodynamic trap experiment[20] is probably the most accurate, and a recent version of the free-fall tube type of apparatus[18] has the highest experiment repetition rate (5 measurements/s).

We compared our nucleation rates against the most recent data from the electrodynamic trap experiment[47] in Fig. 8. The agreement is very good, and the sets of data are of comparable quality. Our absolute accuracy is worse, but we expect that the accuracy will improve though the use of a full computational fluid dynamic model for the modeling of temperature, and through careful selection of microfluidic devices that have very stable temperature PRTDs. Our measurement spans about the same range in temperature (~1.5 °C), but produces data with less noise, all while having a data acquisition rate that we estimate to be at least two orders of magnitude faster. The data acquisition rate was 55 measurements/s for pure water, and 75 measurements/s for silver iodide dispersions.

The free-fall drop ice nucleation instrument[18] is closely related to our apparatus in its approach to making measurements at a high rate of repetition: in this setup a piezoelectric nozzle produces monodisperse water drops that fall at terminal velocity inside a tube that is colder at the bottom, so that the drops are cooled until they freeze. The free-fall apparatus generates drops at a high rate but to record a complete freezing position distribution multiple movies have to be recorded because the field of view of the imaging system is smaller than the range of freezing positions. This fact reduces the effective rate at which the instrument generates data by a factor equal to the number of movies necessary to cover the whole freezing range, and it might increase the noise of the measurements; the measurement noise of the free-fall setup is significantly higher than the noise of our instrument.

After the submission of this paper, Edd *et al.* reported a different microfluidic instrument for the study of ice nucleation.[54] This instrument produced drops of water with identical diameters in liquid fluorocarbon. Approximately 100 drops were trapped in pockets along a microfluidic channel, and all drops were cooled simultaneously by a commercial temperature-controlled plate. This static-drop instrument had a temperature control system that had a very good resolution (0.01 °C) and could be programmed automatically, but the setup lacked an accurate temperature measurement system. The rates of homogenous ice nucleation reported by the static-drop instrument were significantly different than the rates reported by us and by the electrodynamic trap instrument; these rates correspond to a temperature offset of approximately −1.5 °C which could be caused by a systematic error of the measurement of temperature. Compared to the static-drop apparatus our instrument has better accuracy in estimations of temperature, produces two orders of magnitude more data in a cooling cycle, and acquires data 100 times more rapidly; the static-drop instrument has the advantage of having a simpler design and therefore being easier to replicate.

Potential disadvantages of the microfluidic apparatus

One potential disadvantage of our setup is the fact that the drops are in contact with another liquid phase. In principle this phase might influence the freezing process, either by dissolving partially in water (and changing the rate of nucleation), or by causing ice nucleation to start at the water-fluorocarbon interface (rather

than in the volume of the drop). Here we have shown that the rates of nucleation are equal, within experimental uncertainity, to those measured in drops surrounded by air, but did not prove that ice nucleation occurs in the volume of the drop. Encapsulating the drops in fluorocarbon has the advantage of blocking evaporation losses; evaporation is a source of errors because it reduces the volume of the drops, and lowers their temperature.

In our experiment, the drops were subjected to very fast cooling rates, from 2 to 100 °C/s. While this allowed us to measure higher nucleation rates than in other experiments, this cooling rate might be too rapid for the study of heterogeneous nucleation, which occurs more slowly than homogenous nucleation, and sometimes with two-step kinetics.[55,56] The microfluidic technology allows a lot of flexibility in design and we believe that a microfluidic device with rates of cooling of drops typical to cold-plate experiments (from 1 °C/s to 1 °C/min; such cooling rates are typical for clouds and therefore relevant to the study of atmospheric precipitation) can be built. It might not be possible, however, to achieve such rates using our particular setup (*i.e.*, the cold plate and the imaging system that we described here).

Microfluidic technology, a versatile platform for nucleation experiments

Previous ice nucleation instruments that were designed for automated repeated measurement of freezing temperatures in single samples of water[18,20,43,57] cannot vary parameters such as the volume of the sample, or the cooling rates, over a wide (*i.e.* orders of magnitude) range. Here we reported the freezing of water drops having diameters from 55 μm to 180 μm, and we made measurements at cooling rates ranging from ~2 °C/s to ~100 °C/s. These ranges barely touch the potential of microfluidic technology. Using microfluidic flow-focusing generators to generate drops of water in a liquid fluorocarbon, we produced monodisperse drops with diameters ranging from 10 μm to 1 mm, at generation frequencies ranging from ~1 drop/s to ~10 000 drops/s.[58] We believe that the range of the rates of cooling could be expanded by orders of magnitude, on both the low and the high ends of the range we reported here.

Using the apparatus for other processes with fast kinetics

The microfluidic ice nucleation setup provided an experimental platform that might be used to characterize other phenomena characterized by fast kinetics. One obvious example is the kinetics of solid nucleation in supercooled liquids. In general, as long as the change in the substance inside the drop (such a fast chemical reaction) is dependent on temperature, and results in a change in the optical properties of the substance, it can be investigated using our setup if it occurs within the temperature range that we can access (−45 °C to 50 °C).

Experiment complexity and ease of duplication

The integration a microfluidic chip with a sophisticated system for temperature control and measurement system produced a setup for the study of the nucleation of ice that is significantly more complex, and requires more skill to operate, than most lab-on-a-chip applications. The microfluidic system, by itself, is straightforward to build; it is the temperature measurement and control systems that are difficult. The most time-consuming parts of the development of the instrument were the building of the seven-zone plate and the development of the temperature readout system; replicating this design, based on the specifications we describe, should take approximately one year. This relatively long duration would be caused by these factors: i) the device-building process involves steps (sensor fabrication; integration of the sensors in the microfluidic device; making ~100 wire connections to each device) that are time-consuming and require a few trials before they work reliably, and ii) the measurement of temperature with high accuracy is in general difficult; the readout and conversion of electrical resistance to temperature, and the calibration of the devices require not only a complex software, but also a good understanding of the sources of errors (*e.g.* the electrical noise, and the uncertainty of the properties of the fluids) affecting the measurement.

The development of an ice nucleation instrument based on microfluidics does not have to be as difficult as the one we described here. We expect that in the future multiple-zone controlled-temperature plates and thermometer arrays for microfluidic applications will become commercially available, and such commercial availability would obviously make the replication of our setup easier. If the components for the control and measurement of temperature can be purchased, we expect that a skilled scientist would need approximately one year of work to replicate our complete setup. Our design would be simplified considerably if the arrays of thermometers were not used. In this case the temperature would be measured using thermal modeling which uses the temperatures of the cooling plate as boundary conditions; while it is likely that accuracy of the measurement would degrade, the results can be corrected by comparison with results from an experiment that uses embedded thermometers.

A microfluidic system which freezes drops of liquid in another liquid phase, but does not measure the temperatures at which freezing occurs, would be much easier to build. Our work and a previous investigation of freezing of drops in microfluidic channels[25] show that a few simple rules must observed: i) the cooling has to be restricted to parts of the chip which are not too close to the inlets or the outlets of the channels, ii) the system should be able to cool the drops well below the freezing temperature because supercooling might occur, and iii) if the drops will be transported inside the device after freezing, they must be spherical in shape and smaller than the dimensions of the channels.

Conclusion

This paper describes the development of a microfluidic apparatus for the investigation of nucleation of ice in drops of water; the apparatus measures the temperature at which the drops freeze. The main advantage of this apparatus, compared to previous designs, is its very high data throughput: almost two orders of magnitude faster than the current state of the art in ice nucleation instruments. The data sets that the apparatus can record are very large, and that presented here is the largest set of homogenous freezing temperatures ever reported. For this apparatus, we developed a temperature control and measurement system based on a seven-zone temperature-control plate and on two

19-element microfabricated thermometer arrays. This system can measure the temperature of the drops with very low noise, high accuracy, and high speed; to our knowledge it is the most accurate non-invasive temperature measurement system for drop microfluidics.

This project is part of an exploration of metastable liquids using microfluidic technology. We anticipated that microfluidics, and in particular microfluidics involving drops, would be very well suited for investigation of metastable fluids. Working with small volumes of substances reduces the chances of heterogeneous nucleation, and because the time required for preparing the system (*e.g.*, by cooling) can be very short, it is possible to probe deeper into the metastable regime than experiments that investigate larger samples of metastable fluids. Along with the other microfluidic ice nucleation setup,[54] and with recent work that reports the use of microfluidics to study the kinetics of crystallization from supersaturated aqueous solutions,[59] and to produce and study water under tension,[60] this research pioneers the use of microfluidic systems with metastable liquids. The microfluidic-based ice nucleation apparatus achieved, in its first generation, levels of reliability and performance that are comparable or better than the current state-of-the-art. Our experimental platform has the necessary qualities to become an important tool for the study of metastable liquids in general, and of supercooled water in particular.

Acknowledgements

The authors thank Sindy Tang for experimental assistance, Ji Feng for stimulating discussions, and Felice Frankel for assistance with the graphics. This work was supported primarily by the US Department of Energy under award DE-FG02-OOER45852. Shared facilities funded by NSF under MRSEC award DMR-0820484 were utilized for some of the work.

References

1 P. G. Debenedetti, *Metastable Liquids: Concepts and Principles*, Princeton University Press, Princeton, NJ, 1996.
2 H. R. Pruppacher and J. D. Klett, *Microphysics of clouds and precipitation*, D. Reidel Publishing Company, Dodrecht, Holland, 1978.
3 R. H. M. Hatley, F. Franks and H. Day, *Biophys. Chem.*, 1986, **24**, 187–192.
4 R. H. M. Hatley, F. Franks, H. Day and B. Byth, *Biophys. Chem.*, 1986, **24**, 41–46.
5 R. H. M. Hatley, F. Franks and S. F. Mathias, *Process Biochem.*, 1987, **22**, 169–172.
6 H. R. Pruppacher, *J. Atmos. Sci.*, 1995, **52**, 1924–1933.
7 S. C. Mossop, *Proc. Phys. Soc. Lond. B*, 1955, **68**, 193–208.
8 E. K. Bigg, *Proc. Phys. Soc. Lond. B*, 1953, **66**, 688–694.
9 E. J. Langham and B. J. Mason, *Proc. R. Soc. Lond. Ser. A*, 1958, **247**, 493–504.
10 F. Broto and D. Clausse, *J. Phys. C*, 1976, **9**, 4251–4257.
11 D. H. Rasmussen, A. P. Mackenzie, C. A. Angell and J. C. Tucker, *Science*, 1973, **181**, 342–344.
12 P. Taborek, *Phys. Rev. B*, 1985, **32**, 5902–5906.
13 B. M. Cwilong, *Proc. R. Soc. Lond. Ser. A*, 1947, **190**, 137–143.
14 V. J. Schaefer, *Science*, 1946, **104**, 457–459.
15 V. J. Schaefer, *Chem. Rev.*, 1949, **44**, 291–320.
16 D. E. Hagen, R. J. Anderson and J. L. Kassner, *J. Atmos. Sci.*, 1981, **38**, 1236–1243.
17 I. E. Kuhns and B. J. Mason, *Proc. R. Soc. Lond. Ser. A*, 1968, **302**, 437–452.
18 S. E. Wood, M. B. Baker and B. D. Swanson, *Rev. Sci. Instrum.*, 2002, **73**, 3988–3996.
19 S. Bauerecker, P. Ulbig, V. Buch, L. Vrbka and P. Jungwirth, *J. Phys. Chem. C*, 2008, **112**, 7631–7636.
20 B. Kramer, O. Hubner, H. Vortisch, L. Woste, T. Leisner, M. Schwell, E. Ruhl and H. Baumgartel, *J. Chem. Phys.*, 1999, **111**, 6521–6527.
21 S. L. Anna, N. Bontoux and H. A. Stone, *Appl. Phys. Lett.*, 2003, **82**, 364–366.
22 Z. Y. Chen, J. Wang, S. Z. Qian and H. H. Bau, *Lab Chip*, 2005, **5**, 1277–1285.
23 G. Maltezos, M. Johnston and A. Scherer, *Appl. Phys. Lett.*, 2005, **87**.
24 S. Matsuoka, A. Hibara, M. Ueno and T. Kitamori, *Lab Chip*, 2006, **6**, 1236–1238.
25 A. E. Sgro, P. B. Allen and D. T. Chiu, *Anal. Chem.*, 2007, **79**, 4845–4851.
26 The division of the cold zone into five zones represents a design compromise between the spatial resolution of the temperature control (which improves with more zones) and the complexity of the plate.
27 Our first experiments, which include the ones for the data shown in Fig. 6, used a three-zone plate. We later abandoned this design because it did not provide enough flexibility in setting the cooling conditions.
28 With the Peltier elements off, the cold zones reached temperatures of -30 to -35 °C when the heat exchanger had a temperature of -60 °C, because of heating from the lab environment.
29 We limited the maximum temperature of any zone to 50 °C to protect the Peltier elements, which were sealed in-house with silicone (PDMS) to prevent water condensation during operation at low temperatures. The silicone expansion at high temperatures is large enough to cause irreversible mechanical damage to the elements.
30 C. A. Mack, *Fundamental Principles of Optical Lithography: The Science of Microfabrication*, John Wiley & Sons, Chichester, West Sussex, England, 2008.
31 Typically one or two of the 19 sensors in an array were not functional due to fabrication errors.
32 *Low Level Measurements Handbook*, Keithley Instruments, Inc., Cleveland, OH, 2004. Available online at http://www.keithley.com/knowledgecenter.
33 D. C. Duffy, J. C. McDonald, O. J. A. Schueller and G. M. Whitesides, *Anal. Chem.*, 1998, **70**, 4974–4984.
34 The solubility values we list here were reported by the SciFinder Scholar software. These values are numerical estimates, and were originally evaluated using Advanced Chemistry Development (ACD/Labs) software.
35 C. A. Stan, S. K. Y. Tang and G. M. Whitesides, *Anal. Chem.*, 2009, **81**, 2399–2402.
36 The standard deviation of the observed diameter was comparable to the pixel resolution of the image, and was therefore approximately equal to the minimum standard deviation that we could measure.
37 H. Kinoshita, S. Kaneda, T. Fujii and M. Oshima, *Lab Chip*, 2007, **7**, 338–346.
38 We measured optical resolutions using a resolution target (Edmund Optics, USAF target). The smallest resolution measurable with this target was 4.4 μm.
39 G. F. Bolling and W. A. Tiller, *J. Appl. Phys.*, 1961, **32**, 2587–2605.
40 H. R. Pruppacher, *J. Chem. Phys.*, 1967, **47**, 1807–1813.
41 G. Vali, *Atmos. Chem. Phys.*, 2008, **8**, 5017–5031.
42 G. Vali and E. J. Stansbury, *Can. J. Phys.*, 1966, **44**, 477.
43 B. Vonnegut and M. Baldwin, *J. Clim. Appl. Meteorol.*, 1984, **23**, 486–490.
44 C. Marcolli, S. Gedamke, T. Peter and B. Zobrist, *Atmos. Chem. Phys.*, 2007, **7**, 5081–5091.
45 The drop temperature along the channel had a minimum value of -37.8 °C. We discarded from analysis drops that froze while having a cooling rate slower than -2 °C/s, or while being heated, plus the 'frozen-entry' and 'liquid-exit' drops for which we had no freezing temperature information.
46 Eq. (5) is applicable for longer time intervals than eq. (1) and does not restrict N_F to be small compared to N_L.
47 P. Stockel, I. M. Weidinger, H. Baumgartel and T. Leisner, *J. Phys. Chem. A*, 2005, **109**, 2540–2546.
48 This mechanism of heterogeneous ice nucleation, in which the impurity inside the sample of water initiates the nucleation, is

sometimes called 'immersion mode' nucleation, to distinguish it from other mechanisms (*e.g.* the 'contact mode' nucleation – which is due to the contact between an impurity particle and a drop).
49 B. Vonnegut, *J. Appl. Phys.*, 1947, **18**, 593–595.
50 G. R. Edwards and L. F. Evans, *Trans. Faraday Soc.*, 1962, **58**, 1649–1655.
51 R. Gobinathan and P. Ramasamy, *Mater. Res. Bull.*, 1983, **18**, 593–600.
52 We discarded from analysis unfrozen drops, and we did not calculate the freezing rate if the number of freezing events in a temperature bin was less than four.
53 T. Koop, *Z. Phys. Chem.*, 2004, **218**, 1231–1258.
54 J. F. Edd, K. J. Humphry, D. Irimia, D. A. Weitz and M. Toner, *Lab Chip*, 2009, **9**, DOI: 10.1039/b821785h.
55 T. Koop, B. P. Luo, U. M. Biermann, P. J. Crutzen and T. Peter, *J. Phys. Chem. A*, 1997, **101**, 1117–1133.
56 I. Weidinger, J. Klein, P. Stockel, H. Baumgartel and T. Leisner, *J. Phys. Chem. B*, 2003, **107**, 3636–3643.
57 A. F. Heneghan and A. D. J. Haymet, *J. Chem. Phys.*, 2002, **117**, 5319–5327.
58 The flow-focusing generators have higher generation frequencies as their dimension, and therefore the dimension of the drops, becomes smaller.
59 J. Leng and J. B. Salmon, *Lab Chip*, 2009, **9**, 24–34.
60 T. D. Wheeler and A. D. Stroock, *Nature*, 2008, **455**, 208–212.